

# Enzyme-free glucose sensor using a glassy carbon electrode modified with reduced graphene oxide decorated with mixed copper and cobalt oxides

Su-Juan Li<sup>1</sup> · Lin-Lin Hou<sup>1</sup> · Bai-Qing Yuan<sup>1</sup> · Meng-Zhu Chang<sup>1</sup> · Yu Ma<sup>1</sup> · Ji-Min Du<sup>1</sup>

Received: 9 January 2016 / Accepted: 5 March 2016 / Published online: 14 March 2016  
© Springer-Verlag Wien 2016

**Abstract** We describe a binary porous catalyst consisting of a reduced graphene oxide (rGO) support decorated with mixed Cu-Co oxides. It was synthesized electrochemically and characterized by scanning electron microscopy, energy dispersive X-ray spectroscopy and cyclic voltammetry. The nanocomposite was deposited on a glassy carbon electrode (GCE) where it exhibits better electrocatalytic activities for glucose oxidation compared to GCEs modified with CuO<sub>x</sub> or CoO<sub>x</sub> only on an rGO support. The improved electrocatalytic activities are believed to result from the synergistic effect of CuO<sub>x</sub>-CoO<sub>x</sub> binary catalyst, the high conductivity of rGO support, and the porous scaffold. The amperometric sensor, operated in 0.1 M NaOH at a working potential of +0.5 V (vs. SCE), displays a calibration plot for glucose that is linear in the 5 to 570 μM concentration range, and the detection limit is 0.5 μM. The performance of the sensor was evaluated by determination of glucose in (spiked) human urine.

**Keywords** Nanocomposite · Nanoporous material · Nonenzymatic sensing · Binary catalyst · Electrocatalytic oxidation · Cyclic voltammetry · Scanning electron microscopy · Energy dispersive X-ray spectroscopy

## Introduction

Glucose is the primary source of energy for the body and its determination has important significance in clinical diagnosis, health protection and control of food production processes [1]. The increasing demand for glucose sensors with high sensitivity and stability, fast response, low cost, excellent selectivity and reproducibility has driven tremendous research efforts from analytical scientists. Among various glucose sensors, the commercial enzymatic sensors are promising due to their simple equipment, convenient operation, good selectivity and high sensitivity for glucose detection [2]. However, owing to the intrinsic nature of enzymes, enzymatic glucose sensors are often limited by their instability, high cost, complicated immobilization procedures, and critical operating conditions [3, 4]. As an alternative strategy to avoid the above-mentioned drawbacks, enzyme-free glucose sensors have aroused enormous interest and several reviews have summarized the recent advances in this field [5, 6].

The advancement for enzyme-free glucose sensors strongly depend on research into high performance electrode material. So far, noble metals (Pd, Pt, Au) and their alloys [7–10], transition metal or their oxides (Ni or NiO, CuO or Cu<sub>2</sub>O, Co<sub>3</sub>O<sub>4</sub>, MnO<sub>2</sub>, Fe<sub>3</sub>O<sub>4</sub>) [11–23] have been reported as electrode modifications. The high-cost noble metals (such as Pt) can perform in neutral pH values for glucose sensing, which is fascinating for blood glucose monitor. However, they often suffer from very slow kinetics, and the surfaces of which are easily poisoned by adsorbed chloride ions and chemisorbed intermediates that originate from the glucose oxidation process, resulting in decreased sensitivity and poor operational stability [5]. Therefore, increasing attention has been focused on fabricating high-performance enzyme-free devices using inexpensive and resourceful transition-metal catalysts due to their high electrocatalytic activity, good stability, low cost, abundance and high anti-poisoning resistance toward intermediate compounds and

✉ Su-Juan Li  
lemontree88@163.com

<sup>1</sup> Key Laboratory for Clearer Energy and Functional Materials of Henan Province, College of Chemistry and Chemical Engineering, Anyang Normal University, Anyang, Henan 455000, China

chloride ions. Graphene have been widely used as scaffolds for loading of monometallic electrocatalysts for biosensing applications [24–28]. Another alternative is binary electrocatalyst prepared from two different metals, which are also drawing much research interest because of their better catalytic activities and anti-interference ability for glucose detection than their corresponding monometallic counterparts due to the synergistic enhancement effect of two metallic materials. Recently, Awad's group developed a binary catalyst of  $\text{NiO}_x/\text{MnO}_x$  as an anode for an amplified electrochemical oxidation of glucose in alkaline solutions [29]. Yuan et al. reported  $\text{Cu}_2\text{O}/\text{NiO}_x/\text{graphene oxide}$  modified electrode for the enhanced electrochemical oxidation of reduced glutathione and nonenzymatic glucose sensor [30]. Wang et al. developed Ni-Co nanostructures coated reduced graphene oxide nanocomposites electrode for nonenzymatic glucose biosensing [31]. Dong et al. prepared graphene foam loaded nickel-cobalt hydroxides nanoflakes ( $\text{Ni}_x\text{Co}_{2x}(\text{OH})_{6x}/\text{graphene foam}$ ) and showed its superior capability for applications in supercapacitor and electrochemical sensor [32]. These results indicate that the rational design and optimal component for preparation of binary catalyst is important in achieving high-performance electrochemical sensors.

We present a binary catalyst of Cu-Co oxides decorated reduced graphene oxide ( $\text{CuO}_x\text{-CoO}_x/\text{rGO}$ ) composites synthesized by a facile two-step electrochemical approach and demonstrated its application in enzyme-free glucose sensors. In the first step, the bimetallic Cu-Co/rGO composites was firstly fabricated by solution-casting of graphene oxide (GO) nanosheets on glassy carbon electrode, followed by simultaneous electrochemical reduction of GO and electrodeposition of Cu-Co binary nanostructures on it. In the second step, the resultant Cu-Co/rGO composites were subjected to be oxidized in situ into  $\text{CuO}_x\text{-CoO}_x/\text{rGO}$  composites by the cyclic potential sweep technique. The present strategy for the synthesis of  $\text{CuO}_x\text{-CoO}_x/\text{rGO}$  composites by direct electrochemical method endows the intimate contact between the electroactive materials and the current collector, which facilitates the diffusion of active species and the transport of electrons. The electrocatalytic properties of the fabricated  $\text{CuO}_x\text{-CoO}_x/\text{rGO}$  composites modified electrode for glucose oxidation were systematically assessed. Our results showed that the  $\text{CuO}_x\text{-CoO}_x/\text{rGO}$  composites demonstrated better electrocatalytic activities toward glucose oxidation in comparison with those of only  $\text{CuO}_x$  or  $\text{CoO}_x$  on rGO sheets. Therefore, due to the synergistic effect of  $\text{CuO}_x$  or  $\text{CoO}_x$  and the highly electrical conductivities of rGO, a  $\text{CuO}_x\text{-CoO}_x/\text{rGO}$  nanocomposites based enzyme-free glucose sensor was fabricated, which showed good performances for glucose detection, including high sensitivity, good stability, fast response, and excellent selectivity. Importantly, the simple and facile fabrication method of the present sensor makes it competitive to other glucose sensors.

## Experimental

### Reagents and apparatus

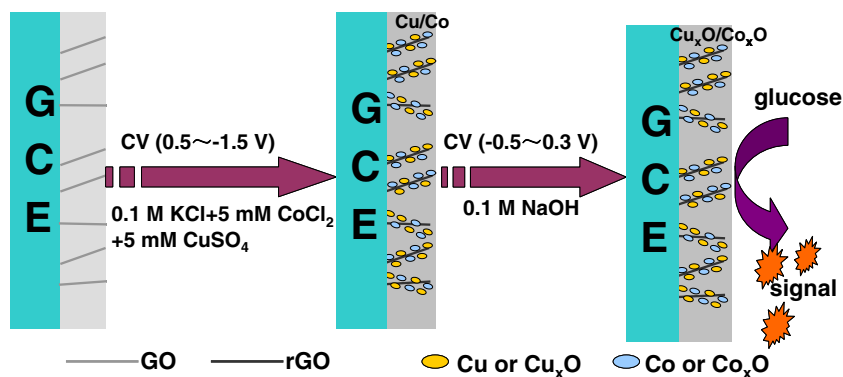
GO was purchased from Nanjing XFNANO Materials Tech Co., Ltd. (China, <http://www.xfnano.com/>). Glucose and interference species were purchased from Sigma-Aldrich (<http://www.sigmaaldrich.com/china-mainland.html>).  $\text{CuSO}_4\cdot 5\text{H}_2\text{O}$ , Cobalt (II) chloride anhydrous, KCl, NaOH and  $\text{H}_2\text{O}_2$  were purchased from Sinopharm Chemical Reagent Co., Ltd. (Shanghai, China, <http://www.sinoreagent.com.cn/>). All of these reagents were of analytical grade and used as received. Unless otherwise stated, ultrapure water (18.2 M $\Omega$  cm) produced by a Milli-Q system was used as the solvent throughout this work.

Scanning electron microscopy (SEM) and energy dispersive X-ray spectroscopy (EDS) were conducted by EDS-integrated JSM-6701F (Japan, <http://www.jeol.cn/>) for surface morphology observations and surface elemental composition analysis. Electrochemical experiments were performed on a CHI 660D electrochemical station (Shanghai Chenhua, China, <http://chi.instrument.com.cn>) with a conventional three-electrode system. The  $\text{CuO}_x\text{-CoO}_x/\text{rGO}$  modified glassy carbon electrode ( $\text{CuO}_x\text{-CoO}_x/\text{rGO}/\text{GCE}$ ) was used as the working electrode. A Pt wire and a saturated calomel electrode (SCE) acted as the counter and reference electrodes, respectively.

### Fabrication of $\text{CuO}_x\text{-CoO}_x/\text{rGO}$ modified electrode

The obtained GO was dispersed in water, giving a yellow-brown dispersion with a concentration of 1 mg mL<sup>-1</sup> by an ultrasonic technique. A 10  $\mu\text{L}$  portion of the resulting GO dispersion was dropped onto a pretreated bare GCE and dried at room temperature to obtain the GO modified GCE (GO/GCE). Here, prior to the surface modification, GCE was polished with 0.3 and 0.05  $\mu\text{m}$  alumina slurries respectively, and then ultrasonically cleaned with ethanol and double distilled water for 10 min to remove the physically adsorbed substance. Next, the electrochemical reduction of GO on electrode surface and the simultaneous electrodeposition of Cu and Co nanostructures were performed in a 0.1 M KCl aqueous solution containing 5 mM  $\text{CoCl}_2$  and 5 mM  $\text{CuSO}_4$  in the potential range from 0.5 to  $-1.5$  V (vs. SCE) for 10 cycles at a scan rate of 50 mV s<sup>-1</sup> by cyclic voltammetry (CV). The electrode prepared in this step was denoted as Cu-Co/rGO composites modified electrode. The electrode was then rinsed several times with water and dried with a flow of  $\text{N}_2$  before it was repeatedly scanned in a 0.1 M NaOH with CV under the potential range of  $-0.5$  to 0.3 V at 50 mV s<sup>-1</sup> for 60 cycles, allowing the Cu-Co nanostructures to be oxidized into  $\text{CuO}_x\text{-CoO}_x$  nanostructures. The whole process for preparation of  $\text{CuO}_x\text{-CoO}_x/\text{rGO}/\text{GCE}$  is illustrated in Scheme 1. For

**Scheme 1** Schematic illustration for the fabrication and application of  $\text{CuO}_x\text{-CoO}_x/\text{rGO}$  modified glassy carbon electrode (GCE) for glucose sensor. GO and rGO in the scheme are the acronyms of graphene oxide and reduced graphene oxide



comparison,  $\text{CuO}_x/\text{rGO}/\text{GCE}$  and  $\text{CoO}_x/\text{rGO}/\text{GCE}$  were prepared in deposition solutions of 0.1 M KCl + 10 mM  $\text{CuSO}_4$  and 0.1 M KCl + 10 mM  $\text{CoCl}_2$ , respectively, by the similar procedure as described above. The total electrolyte concentration was also maintained as 10 mM to minimize the difference about deposition conditions but highlighted the component difference between monometallic oxides/rGO/GCE and bimetallic oxides/rGO/GCE (deposition solutions of 0.1 M KCl + 5 mM  $\text{CuSO}_4$  + 5 mM  $\text{CoCl}_2$ ).

### Electrochemistry measurements

Cyclic voltammetry (CV) and amperometric experiments were carried out at room temperature. A certain volume of stock solution of glucose and 10 mL supporting electrolyte were added into an electrochemical cell, and then the three-electrode system was inserted into the cell. The CV was carried out to investigate the electrochemical response of the modified electrode toward glucose. The amperometric experiment was performed to achieve the quantitative analysis.

## Results and discussion

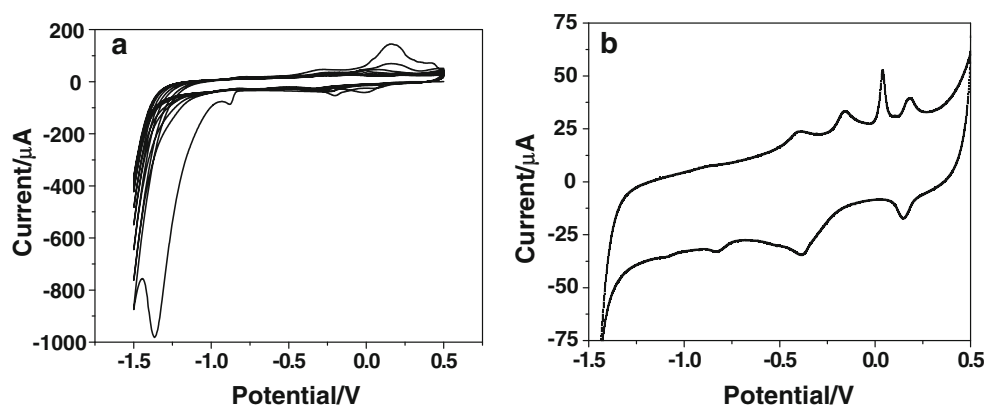
### Formation mechanism and characterization of $\text{CuO}_x\text{-CoO}_x/\text{rGO}$ composites

The Cu-Co binary catalyst was prepared on GO/GCE by CV technique in the first step. Figure 1 shows the cyclic voltammograms (CVs) of the GO/GCE scanned in 0.1 M KCl solution containing 5 mM  $\text{CoCl}_2$  and 5 mM  $\text{CuSO}_4$  at a potential range from 0.5 to -1.5 V for 10 cycles. As observed, there is a large cathodic peak at -1.36 V in the first cycle due to reduction of the high number of oxygen-containing functional groups in GO. With further increasing the scanning cycles, the cathodic currents decrease considerably and disappear after several potential cycles, indicating that GO has been electrochemically reduced to rGO [33–35]. The obvious reduction peak at -0.88 V in the first cycle is resulted from the reduction of  $\text{Co}^{2+}$  to  $\text{Co}(0)$ , which is accordance with previous results

[31, 36]. The two redox peaks located at -0.20/0.17 V and -0.01/0.43 V are corresponded to the conversion between three different valence state of copper of  $\text{Cu}(0)$ ,  $\text{Cu}(I)$  and  $\text{Cu}(II)$ . The current decrease of both characteristic peak of  $\text{Co}$  and  $\text{Cu}$  with increasing cycle number indicated that  $\text{Co}^{2+}$  and  $\text{Cu}^{2+}$  have been reduced and deposited on the surface of rGO/GCE slowly. After the resultant electrode was subjected to be scanned in NaOH with CV for oxidizing binary Cu-Co to form  $\text{CuO}_x\text{-CoO}_x/\text{rGO}$  composites, the obtained  $\text{CuO}_x\text{-CoO}_x/\text{rGO}/\text{GCE}$  was scanned in 0.1 M NaOH solution under the potential range from -1.5 to 0.5 V to characterize the successful deposition of binary  $\text{CuO}_x\text{-CoO}_x$  on rGO surface. As shown in Fig. 1b, it is clear that several anodic and cathodic peaks appeared, among which the anodic peaks at -0.40 and -0.15 V represent the conversion of  $\text{Cu}(0)$  to  $\text{Cu}(I)$  and  $\text{Cu}(I)$  to  $\text{Cu}(II)$ , respectively. The corresponding cathodic peaks at -0.38 and -0.84 V are attributed to the transition of  $\text{Cu}(II)$  to  $\text{Cu}(I)$  and of  $\text{Cu}(I)$  to  $\text{Cu}(0)$ , respectively. This typical redox peaks of copper is very similar to those of previous results [37, 38]. Furthermore, the other two anodic peaks at 0.04 and 0.18 V and the cathodic peak at 0.15 V corresponds to the conversion between different cobalt phases, such as  $\text{Co}(0)$ ,  $\text{CoO}(II)$  and  $\text{CoOOH}(III)$  [36, 39]. The CV results demonstrate that  $\text{CuO}_x\text{-CoO}_x$  binary catalyst has been successful deposited on rGO support using the present method.

The morphological characterization of the modified electrodes is disclosed by SEM imaging and shown in Fig. 2. Image of Fig. 2a and b show the typical SEM micrographs of  $\text{CuO}_x/\text{rGO}/\text{GCE}$  at different magnifications. It reveals that the  $\text{CuO}_x$  is deposited as nanoparticles in a uniform distribution with an average particle size about 50 nm on wrinkled rGO surface. This average particle size of  $\text{CuO}_x$  was measured from about 100 nanoparticles in Fig. 2a. Figure 2c and d show SEM images of  $\text{CoO}_x/\text{rGO}/\text{GCE}$ . A flower-like shape constituted by several  $\text{CoO}_x$  nanoflakes with thickness of about 20 nm can be deposited on rGO surface. In image of Fig. 2e ( $\text{CuO}_x\text{-CoO}_x/\text{rGO}/\text{GCE}$  sample), a three-dimensional (3D) nanocomposites composed with wrinkled rGO, nanoparticles and nanoflakes were obtained. The  $\text{CoO}_x$  nanoflakes can

**Fig. 1** **a** CVs of GO/GCE in 0.1 M KCl solution containing 5 mM  $\text{CoCl}_2$  and 5 mM  $\text{CuSO}_4$  for 10 cycles, **b** CV of  $\text{CuO}_x\text{-CoO}_x/\text{rGO}/\text{GCE}$  in 0.1 M NaOH solution. The scan rate is  $50 \text{ mV s}^{-1}$



induce the formation of  $\text{CuO}_x$  nanoparticles and thus some aggregated nanoparticles cover with the nanoflakes to form a porous and interconnected network. The obtained 3D porous structures provide probability for enhancing glucose adsorption and facilitating transport of analyte species. The EDX spectra shown in Fig. 2f reveal the presence of the elements oxygen, Cu and Co. This proves the successful deposition of the composite on the surface of rGO.

### Electrocatalytic oxidation of glucose on $\text{CuO}_x\text{-CoO}_x/\text{rGO}$ composites modified electrode

To evaluate the catalytic properties of the binary catalyst in the oxidation of glucose, CVs were recorded for the rGO/GCE (a),  $\text{CoO}_x/\text{rGO}/\text{GCE}$  (b),  $\text{CuO}_x/\text{rGO}/\text{GCE}$  (c) and  $\text{CuO}_x\text{-CoO}_x/\text{rGO}/\text{GCE}$  (d) in 0.1 mol  $\text{L}^{-1}$  NaOH in the absence (black curve) and the presence (red curve) of 5 mM glucose

**Fig. 2** SEM images of  $\text{CuO}_x/\text{rGO}/\text{GCE}$  (a, b),  $\text{CoO}_x/\text{rGO}/\text{GCE}$  (c, d),  $\text{CuO}_x\text{-CoO}_x/\text{rGO}/\text{GCE}$  (e) at different magnification and the EDX spectra of  $\text{CuO}_x\text{-CoO}_x/\text{rGO}/\text{GCE}$  (f)

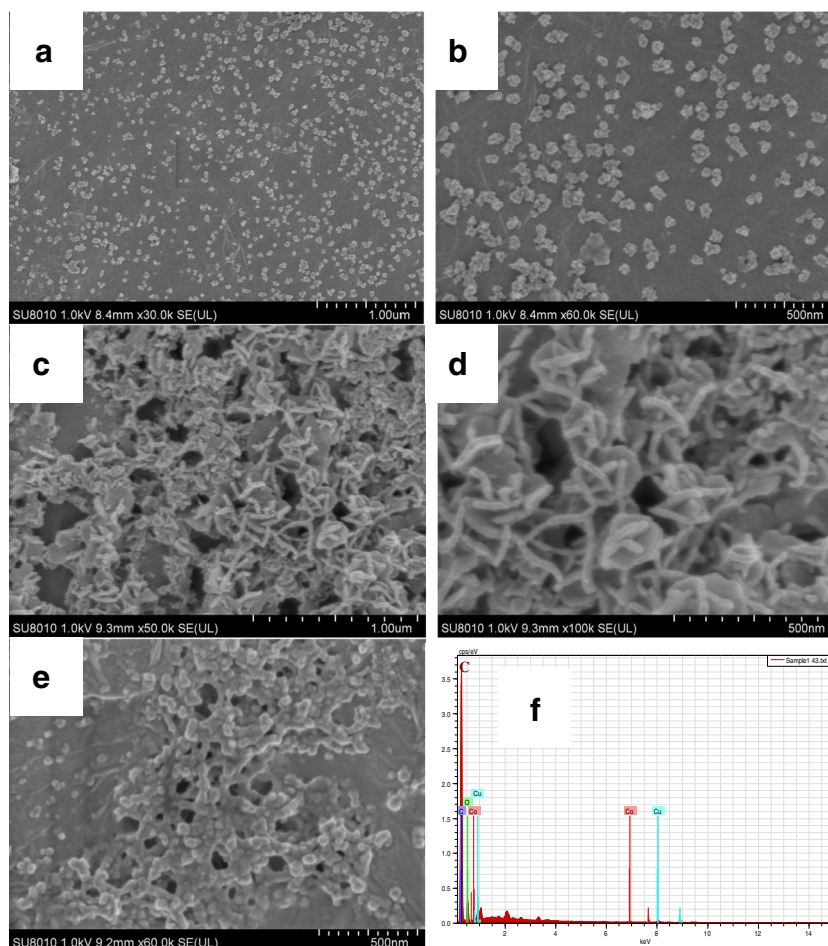
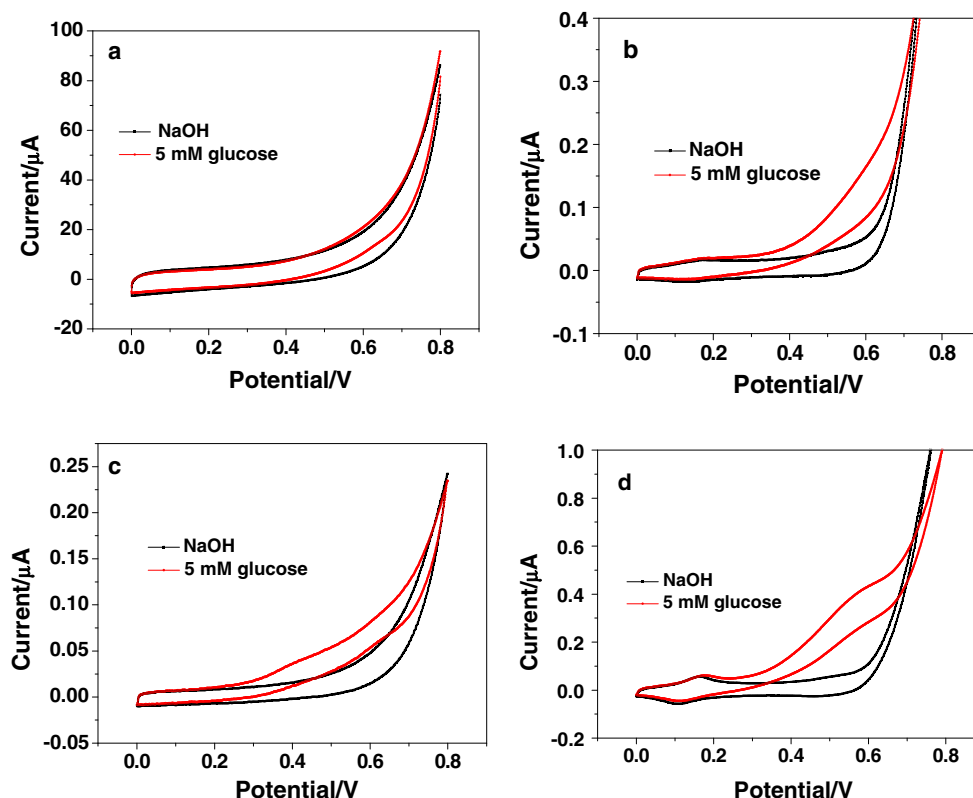




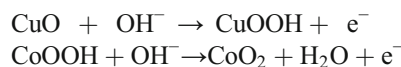
**Fig. 3** CVs of rGO/GCE (a),  $\text{CoO}_x/\text{rGO}/\text{GCE}$  (b),  $\text{CuO}_x/\text{rGO}/\text{GCE}$  (c) and  $\text{CuO}_x\text{-CoO}_x/\text{rGO}/\text{GCE}$  (d) in  $0.1 \text{ mol L}^{-1}$  NaOH in the absence (black curve) and the presence (red curve) of 5 mM glucose at a scan rate of  $50 \text{ mV s}^{-1}$



at a scan rate of  $50 \text{ mV s}^{-1}$  (Fig. 3). As observed from Fig. 3a, no obvious current change upon addition of glucose into blank solution, indicating that the electrocatalytic activities of rGO toward glucose oxidation is limited. The CVs of  $\text{CoO}_x/\text{rGO}/\text{GCE}$  in blank solution shows a redox peak at  $+0.15/+0.17 \text{ V}$ , which corresponds to the redox couples of Co itself. Glucose addition causes an obvious anodic current increase starting at about  $0.30 \text{ V}$  due to the irreversible glucose oxidation catalyzed by  $\text{CoO}_x$  nanoflakes. An observable increase in anodic current, starting at about  $+0.23 \text{ V}$  for  $\text{CuO}_x/\text{rGO}/\text{GCE}$  after the addition of glucose also shows efficient electrocatalytic activities of  $\text{CuO}_x$  nanoparticles toward glucose oxidation. When

the two electrocatalysts were integrated together to form a binary catalyst at  $\text{CuO}_x\text{-CoO}_x/\text{rGO}/\text{GCE}$ , a noticeable and significant increase in anodic current, corresponding to glucose oxidation, starts at about  $+0.19 \text{ V}$ , which is more negative than the monometallic oxides on graphene surface ( $+0.23 \text{ V}$  for  $\text{CuO}_x/\text{rGO}/\text{GCE}$  and  $+0.30 \text{ V}$  for  $\text{CoO}_x/\text{rGO}/\text{GCE}$ ). In addition, the anodic current of 5 mM glucose at  $\text{CuO}_x\text{-CoO}_x/\text{rGO}/\text{GCE}$  is the largest among the four electrodes. All these results demonstrate that the electrocatalytic activity of  $\text{CuO}_x\text{-CoO}_x/\text{rGO}$  composites is greatly enhanced in comparison with those of  $\text{CuO}_x$  or  $\text{CoO}_x$  on rGO sheets due to synergistic enhancement effect.

The oxidation of glucose at the Cu and Co electrodes in an alkaline medium is generally considered a multi-step process, where strongly oxidizing Cu(III) and Co(IV) species ( $\text{CuOOH}$  and  $\text{CoO}_2$ ) are responsible for its electrocatalytic behavior [28, 37]. According to previous results, CuO and  $\text{CoOOH}$  is electrochemically oxidized to Cu(III) and Co(IV) species.



Then, glucose is oxidized by Cu(III) and Co(IV) species to produce glucolactone that finally hydrolyses in aqueous medium to form gluconic acid.

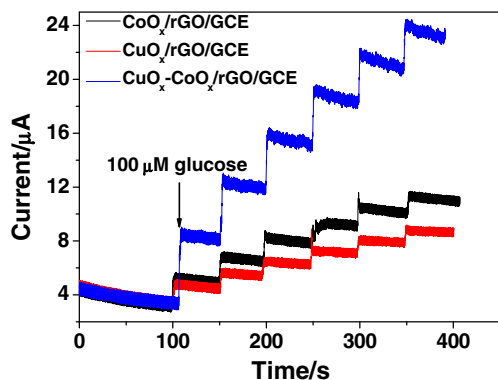
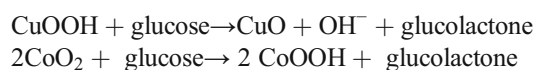
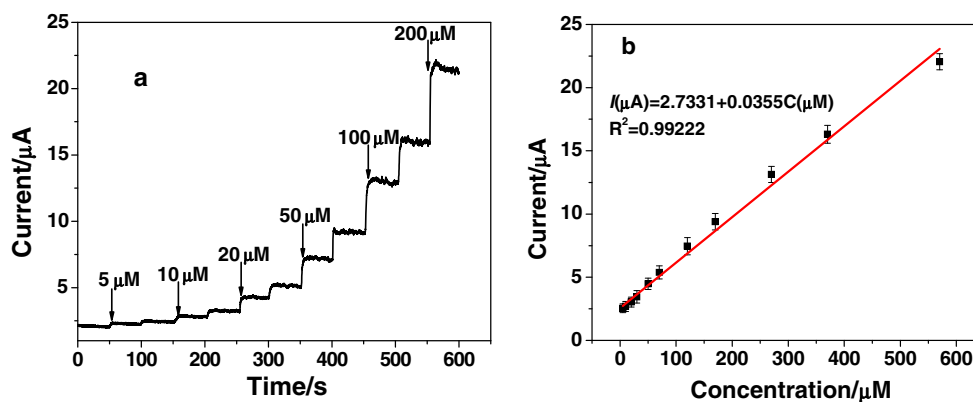


**Fig. 4** The amperometric responses of  $\text{CoO}_x/\text{rGO}/\text{GCE}$ ,  $\text{CuO}_x/\text{rGO}/\text{GCE}$ ,  $\text{CuO}_x\text{-CoO}_x/\text{rGO}/\text{GCE}$  upon the successive additions of  $100 \mu\text{M}$  glucose at applied potential of  $+0.5 \text{ V}$

**Fig. 5** **a** Amperometric response of the  $\text{CuO}_x\text{-CoO}_x/\text{rGO}/\text{GCE}$  (holding at +0.50 V) upon addition of glucose to increasing concentrations in 0.1 M NaOH, **b** The corresponding calibration curve



To further validate the synergistic enhancement effect of electrocatalytic behavior of  $\text{CuO}_x$  and  $\text{CoO}_x$ , amperometric responses of  $\text{CoO}_x/\text{rGO}/\text{GCE}$ ,  $\text{CuO}_x/\text{rGO}/\text{GCE}$  and  $\text{CuO}_x\text{-CoO}_x/\text{rGO}/\text{GCE}$  upon successive additions of 100  $\mu\text{M}$  glucose in 0.1 M NaOH at a constant potential of +0.50 V were recorded in Fig. 4. As observed, the detection sensitivity of glucose at  $\text{CoO}_x/\text{rGO}/\text{GCE}$ ,  $\text{CuO}_x/\text{rGO}/\text{GCE}$  and  $\text{CuO}_x\text{-CoO}_x/\text{rGO}/\text{GCE}$ , was calculated to be 15.98, 10.07 and 42.03  $\mu\text{A } \mu\text{M}^{-1}$ , respectively. The largest response sensitivity for glucose was obtained at  $\text{CuO}_x\text{-CoO}_x/\text{rGO}/\text{GCE}$ , which is consistent with the CV results. Adding the current of  $\text{CoO}_x/\text{rGO}/\text{GCE}$  and  $\text{CuO}_x/\text{rGO}/\text{GCE}$  together, it is found that this value (26.05  $\mu\text{A } \mu\text{M}^{-1}$ ) is still smaller than that of  $\text{CuO}_x\text{-CoO}_x/\text{rGO}/\text{GCE}$  (42.03  $\mu\text{A } \mu\text{M}^{-1}$ ). This further indicates that a synergistic enhancement effect between  $\text{CoO}_x$  and  $\text{CuO}_x$  occurs toward the electrochemical oxidation of glucose. Such enhanced electrocatalytic performance of the  $\text{CuO}_x\text{-CoO}_x/\text{rGO}$  composites may be ascribed to a synergistic effect between  $\text{CuO}_x$  nanoparticles and  $\text{CoO}_x$  nanoflakes, which includes more catalytic active sites for the glucose oxidation. Furthermore, the porous and interconnected network of composites and high conductivity of rGO provide convenient electron transfer channel and highly effective catalytic sites to facilitate the electrooxidation of glucose correspondingly.

#### Amperometric sensing of glucose and interference test

Before quantitative analysis, we investigate the effect of applied potentials (+0.3, +0.4, +0.5, +0.6, +0.7 V) on amperometric currents of 100  $\mu\text{M}$  glucose (data not shown). The results demonstrated that +0.5 and +0.6 V have equal amperometric currents for 100  $\mu\text{M}$  glucose and the current is the largest among all of the above potentials. Considering that the high detection sensitivity as well as the fact that serious interference at high applied potentials, +0.5 V was chosen as the optimum applied potential for glucose detection. Figure 5a presents the amperometric response at the  $\text{CuO}_x\text{-CoO}_x/\text{rGO}$  composites electrode upon addition of glucose to increasing concentrations in 0.1 M NaOH at an applied potential of +0.5 V, from which rapid response to the addition of glucose (within 3 s) can be obtained. The response to glucose shows a good linear range from 5  $\mu\text{M}$  to 570  $\mu\text{M}$  with a correlation coefficient of 0.9922 and a slope of 35.5  $\mu\text{A } \text{mM}^{-1}$  (as shown in Fig. 5b). Based on the previous work described by Shi et al. [40], the electrode surface area of the  $\text{CuO}_x\text{-CoO}_x/\text{rGO}$  composites electrode can be calculated to be about 0.07  $\text{cm}^2$ . The sensitivity of the sensor is calculated to be 507  $\mu\text{A } \text{mM}^{-1} \text{cm}^{-2}$ , which is higher than the reported values at  $\text{Fe}_3\text{O}_4$  nanorod arrays ( $\text{Fe}_3\text{O}_4$  NRAs) electrode (406.9  $\mu\text{A } \text{mM}^{-1} \text{cm}^{-2}$ ) [23],  $\text{CoO}_x\text{NPs}/\text{ERGO}$  modified electrode (79.3  $\mu\text{A } \text{mM}^{-1} \text{cm}^{-2}$ ) [28], RGO- $\text{Ni}(\text{OH})_2$  modified

**Table 1** Comparison of enzyme-free glucose sensing performances based on various nanomaterials

Electrode materials	Response time (s)	Potential (V)	Sensitivity ( $\mu\text{A } \text{mM}^{-1} \text{cm}^{-2}$ )	Linear range (mM)	LOD ( $\mu\text{M}$ )	Reference
$\text{Fe}_3\text{O}_4$ NRAs	<8	+0.6	406.9	0.0005–0.766	0.1	23
$\text{CoO}_x\text{NPs}/\text{ERGO}$	<5	+0.60	79.3	0.01–0.55 mM	2	28
RGO- $\text{Ni}(\text{OH})_2$	<7	+0.54	11.43	0.002–3.1	0.6	41
CuO nanorods	<10	+0.60	371.43	0.004–8 mM	4	42
CoOOH nanosheets	<4	+0.40	341	0.03–0.7 mM	30.9	43
FeOOH nanowires	–	+0.4	12.13	0.015–33 mM	15	44
CuONPs-CSs	<5	+0.55	2981	0.0005–2.3	0.1	45
$\text{CuO}_x\text{-CoO}_x/\text{graphene}$	<3	+0.50	507	0.005–0.570	0.5	This work

electrode ( $11.43 \mu\text{A mM}^{-1} \text{cm}^{-2}$ ) [41], CuO nanorods modified electrode ( $371.43 \mu\text{A mM}^{-1} \text{cm}^{-2}$ ) [42], CoOOH nanosheets modified electrode ( $341 \mu\text{A mM}^{-1} \text{cm}^{-2}$ ) [43], and FeOOH nanowires modified electrode ( $12.13 \mu\text{A mM}^{-1} \text{cm}^{-2}$ ) [44], but lowers that the CuONPs-CSs modified electrode with a sensitivity of  $2981 \mu\text{A mM}^{-1} \text{cm}^{-2}$  [45]. The detection limit at a signal to noise ratio of 3 is estimated to be  $0.5 \mu\text{M}$ . The performance of the prepared  $\text{CuO}_x\text{-CoO}_x/\text{rGO}$  catalyst for glucose sensing is compared with some of existing enzyme-free glucose sensors based on various nanomaterials. As shown in Table 1, it can be concluded that the prepared  $\text{CuO}_x\text{-CoO}_x/\text{rGO}$  catalyst is among the top list of sensors with a faster response speed, a higher sensitivity, and a lower detection limit.

Other species often present along with glucose in biological samples, such as  $\text{H}_2\text{O}_2$ , NaCl, dopamine (DA), ascorbic acid (AA), uric acid (UA) and fructose, may interfere. In the physiological sample, glucose concentration ( $4.4\text{--}6.6 \text{ mM}$ ) is generally much higher than those of interfering species [7–9]. Therefore, the influence of  $0.1 \text{ mM}$  interfering species on the current response of  $1 \text{ mM}$  glucose was evaluated. From the current response in Fig. 6, it can be observed that a remarkable glucose signal was obtained comparing to the other six interfering species. Compared to glucose, all the interfering species yield current response less than  $9.3 \%$ . The results indicate that an acceptable selectivity has been obtained for the present sensor.

#### Repeatability, reproducibility and stability of the sensor

The inter-electrode reproducibility investigation was conducted by comparing the response currents of six independent  $\text{CuO}_x\text{-CoO}_x/\text{rGO}$  modified electrodes prepared under the same conditions. The relative standard deviation (RSD) of response for amperometric determination of  $100 \mu\text{M}$  glucose at  $0.50 \text{ V}$  was  $5.3 \%$ . In addition, four measurements of  $100 \mu\text{M}$  glucose using the same electrode yielded a RSD of  $4.6 \%$ . These results indicated excellent intra-electrode and inter-electrode reproducibility. The long-term stability of electrode was investigated by analyzing its amperometric response after one-month storage. The results showed only  $7.4 \%$  decrease in the current response to  $100 \mu\text{M}$  glucose. The good stability and repeatability make the  $\text{CuO}_x\text{-CoO}_x/\text{rGO}$  modified electrode feasible for practical applications.

#### Determination of glucose in urine

The  $\text{CuO-CoO}/\text{rGO}$  composites modified electrode was applied for the analysis of glucose spiked in the urine. The urine spiked with  $10 \text{ mM}$  and  $20 \text{ mM}$  standard solutions of glucose were signed as sample 1 and 2, respectively. The amperometric detection was carried out at the applied potential of  $0.5 \text{ V}$  in  $10 \text{ mL } 0.1 \text{ mol L}^{-1} \text{ NaOH}$  solution under stirring condition with the injection of  $10 \mu\text{L}$  urine. The quantitative

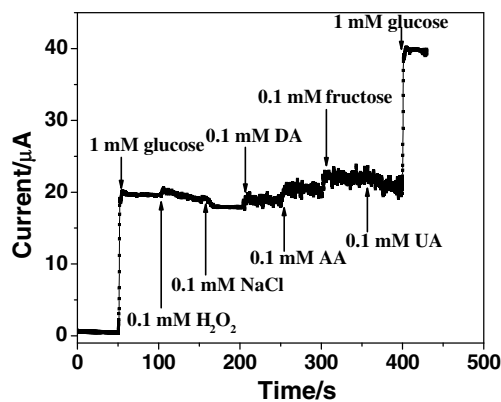


**Fig. 6** Amperometric responses of the  $\text{CuO}_x\text{-CoO}_x/\text{rGO}/\text{GCE}$  to successive additions of  $1 \text{ mM}$  glucose,  $0.1 \text{ mM H}_2\text{O}_2$ ,  $0.1 \text{ mM NaCl}$ ,  $0.1 \text{ mM DA}$ ,  $0.1 \text{ M AA}$ ,  $0.1 \text{ M fructose}$ ,  $0.1 \text{ mM UA}$  and  $1 \text{ mM}$  glucose in  $0.1 \text{ M NaOH}$  at applied potential of  $0.5 \text{ V}$

determination of samples was performed using the standard addition method and the results are shown in Table 2. The recoveries indicate that the sensor can be used for the determination of glucose in urine.

#### Conclusions

In summary, an efficient enzyme-free glucose sensor based on a binary catalyst  $\text{CuO}_x\text{-CoO}_x/\text{rGO}$  was prepared by a direct two-step electrodeposition on electrode surface. The present sensor for glucose possessed good analytical performance, such as low detection limit, high detection sensitivity and reproducibility, acceptable selectivity and low cost. But there are some drawbacks when applied to sensing glucose in real samples. The first is the limited linear range of the present sensor ( $5 \sim 570 \mu\text{M}$ ), which is far from the normal blood glucose concentration. To match the analytical ranges of sensor to real samples, simulated conditions using buffers ( $0.1 \text{ M NaOH}$ ) have to be used in the laboratory. The second is the  $\text{CuO}_x\text{-CoO}_x/\text{rGO}$  based sensor unable to be used in solutions with pH equal to or less than 7 because the electrocatalysis is highly dependent on the presence of  $\text{OH}^-$  anions. Therefore, there is still a long way for the low-cost nonnoble metals based enzyme-free glucose sensor to be used for practical applications. However, we envision that this work will open a new way to fabricate high performance binary nanocomposites as electrode materials and promote their multifunctional applications in biosensor, catalysis and bioengineer related areas.

**Table 2** Amperometric determination of glucose spiked in human urine samples ( $n = 4$ )

Urine samples	Spiked ( $\mu\text{M}$ )	Found ( $\mu\text{M}$ )	R.S.D. (%)	Recovery (%)
Sample 1	10.0	9.68	2.64	96.8
Sample 2	20.0	19.8	2.08	99.0

**Acknowledgments** This work was supported by the Grants from the National Natural Science Foundation of China (21105002, 21273010), the fund project for Young Scholar sponsored by Henan province (14HASTIT012, 13HASTIT014, 2013GGJS-147) and for Henan Key Technologies R&D Program (122102310516, 12B150002) and the Innovative Foundation for the College students of China and Anyang Normal University (201310479012, ASCX/2015-Z14).

**Compliance with Ethical Standards** The author(s) declare that they have no competing interests

## References

- Wang J (2008) Electrochemical glucose biosensors. *Chem Rev* 108: 814–825
- Shi X, Gu W, Li B, Chen N, Zhao K, Xian Y (2014) Enzymatic biosensors based on the use of metal oxide nanoparticles. *Microchim Acta* 181:1–22
- Yang Z, Xu Y, Li J, Jian Z, Yu S, Zhang Y, Hu X, Dionysiou DD (2015) An enzymatic glucose biosensor based on a glassy carbon electrode modified with cylinder-shaped titanium dioxide nanorods. *Microchim Acta* 182:1841–1848
- Devasenathipathy R, Karthik R, Chen S-M, Ali MA, Mani V, Lou B-S, Al-Hemaid FMA (2015) Enzymatic glucose biosensor based on bismuth nanoribbons electrochemically deposited on reduced graphene oxide. *Microchim Acta* 182:2165–2172
- Wang G, He X, Wang L, Gu A, Huang Y, Fang B, Geng B, Zhang X (2013) Non-enzymatic electrochemical sensing of glucose. *Microchim Acta* 180:161–186
- Chen X, Wu G, Cai Z, Oyama M, Chen X (2014) Advances in enzyme-free electrochemical sensors for hydrogen peroxide, glucose, and uric acid. *Microchim Acta* 181:689–705
- Chen X, Tian X, Zhao L, Huang Z, Oyama M (2014) Nonenzymatic sensing of glucose at neutral pH values using a glassy carbon electrode modified with graphene nanosheets and Pt-Pd bimetallic nanocubes. *Microchim Acta* 181:783–789
- Zhao L, Wu G, Cai Z, Zhao T, Yao Q, Chen X (2015) Ultrasensitive non-enzymatic glucose sensing at near-neutral pH values via anodic stripping voltammetry using a glassy carbon electrode modified with Pt<sub>3</sub>Pd nanoparticles and reduced graphene oxide. *Microchim Acta* 182:2055–2060
- Mei H, Wu W, Yu B, Li Y, Wu H, Wang S, Xia Q (2015) Non-enzymatic sensing of glucose at neutral pH values using a glassy carbon electrode modified with carbon supported Co@Pt core-shell nanoparticles. *Microchim Acta* 182:1869–1875
- Ding Y, Liu Y, Parisi J, Zhang L, Lei Y (2011) A novel NiO-Au hybrid nanobelts based sensor for sensitive and selective glucose detection. *Biosens Bioelectron* 2:393–398
- Niu X, Lan M, Zhao H, Chen C (2013) Highly sensitive and selective nonenzymatic detection of glucose using three-dimensional porous nickel nanostructures. *Anal Chem* 85:3561–3569
- Wang G, Lu X, Zhai T, Ling Y, Wang H, Tong Y, Li Y (2012) Free-standing nickel oxide nanoflake arrays: synthesis and application for highly sensitive non-enzymatic glucose sensors. *Nanoscale* 4: 3123–3127
- Yang J, Jiang L-C, Zhang W-D, Gunasekaran S (2010) A highly sensitive non-enzymatic glucose sensor based on a simple two-step electrodeposition of cupric oxide (CuO) nanoparticles onto multi-walled carbon nanotube arrays. *Talanta* 82:25–33
- Hsu Y-W, Hsu T-K, Sun C-L, Nien Y-T, Pu N-W, Ger M-D (2012) Synthesis of CuO/graphene nanocomposites for nonenzymatic electrochemical glucose biosensor applications. *Electrochim Acta* 8:152–157
- Wang G, Wei Y, Zhang W, Zhang X, Fang B, Wang L (2010) Enzyme-free amperometric sensing of glucose using Cu-CuO nanowire composites. *Microchim Acta* 168:87–92
- Mei L-P, Song P, Feng J-J, Shen J-H, Wang W, Wang A-J, Weng X (2015) Nonenzymatic amperometric sensing of glucose using a glassy carbon electrode modified with a nanocomposite consisting of reduced graphene oxide decorated with Cu<sub>2</sub>O nanoclusters. *Microchim Acta* 182:1701–1708
- Yu H, Jian X, Jin J, Zheng X-c, R-t L, G-c Q (2015) Nonenzymatic sensing of glucose using a carbon ceramic electrode modified with a composite film made from copper oxide, overoxidized polypyrrole and multi-walled carbon nanotubes. *Microchim Acta* 182:157–165
- Zhou D-L, Feng J-J, Cai L-Y, Fang Q-X, Chen J-R, Wang A-J (2014) Facile synthesis of monodisperse porous Cu<sub>2</sub>O nanospheres on reduced graphene oxide for non-enzymatic amperometric glucose sensing. *Electrochim Acta* 115:103–108
- Wang A-J, Feng J-J, Li Z-H, Liao Q-C, Wang Z-Z, Chen J-R (2012) Solvothermal synthesis of Cu/Cu<sub>2</sub>O hollow microspheres for non-enzymatic amperometric glucose sensing. *CrystEngComm* 14: 1289–1295
- Hou C, Xu Q, Yin L, Hu X (2012) Metal-organic framework templated synthesis of Co<sub>3</sub>O<sub>4</sub> nanoparticles for direct glucose and H<sub>2</sub>O<sub>2</sub> detection. *Analyst* 137:5803–5808
- Ding Y, Wang Y, Su L, Bellagamba M, Zhang H, Lei Y (2010) Electrospun Co<sub>3</sub>O<sub>4</sub> nanofibers for sensitive and selective glucose detection. *Biosens Bioelectron* 26:542–548
- Chen J, Zhang W-D, Ye J-S (2008) Nonenzymatic electrochemical glucose sensor based on MnO<sub>2</sub>/MWNTs nanocomposite. *Electrochem Commun* 10:1268–1271
- Zhang C, Ni H, Chen R, Zhan W, Zhang B, Lei R, Xiao T, Zha Y (2015) Enzyme-free glucose sensing based on Fe<sub>3</sub>O<sub>4</sub> nanorod arrays. *Microchim Acta* 182:1811–1818
- Sultan SC, Anik U (2014) Gr–Pt hybrid NP modified GCPE as label and indicator free electrochemical genosensor platform. *Talanta* 129:523–528
- Tepeli Y, Anik U (2015) Comparison of performances of bioanodes modified with graphene oxide and graphene–platinum hybrid nanoparticles. *Electrochem Commun* 57:31–34
- Aslan S, Anik U (2016) Microbial glucose biosensors based on glassy carbon paste electrodes modified with gluconobacter oxydans and graphene oxide or graphene–platinum hybrid nanoparticles. *Microchim Acta* 183:73–81
- Li S-J, Xia N, Lv X-L, Zhao M-M, Yuan B-Q, Pang H (2014) A facile one-step electrochemical synthesis of graphene/NiO nanocomposites as efficient electrocatalyst for glucose and methanol. *Sens Actuators B Chem* 190:809–817
- Li S-J, Du J-M, Chen J, Mao N-N, Zhang M-J, Pang H (2014) Electrodeposition of cobalt oxide nanoparticles on reduced graphene oxide: a two-dimensional hybrid for enzyme-free glucose sensing. *J Solid State Electrochem* 18:1049–1056
- El-Refaei SM, Saleh MM, Awad MI (2013) Enhanced glucose electrooxidation at a binary catalyst of manganese and nickel oxides modified glassy carbon electrode. *J Power Sources* 223:125–128
- Yuan B, Xu C, Liu L, Zhang Q, Ji S, Pi L, Zhang D, Huo Q (2013) Cu<sub>2</sub>O/NiO<sub>x</sub>/graphene oxide modified glassy carbon electrode for the enhanced electrochemical oxidation of reduced glutathione and nonenzyme glucose sensor. *Electrochim Acta* 104:78–83
- Wang L, Lu X, Ye Y, Sun L, Song Y (2013) Nickel-cobalt nanostructures coated reduced graphene oxide nanocomposite electrode for nonenzymatic glucose biosensing. *Electrochim Acta* 114:484–493
- Dong S, Dao AQ, Zheng B, Tan Z, Fu C, Liu H, Xiao F (2015) One-step electrochemical synthesis of three-dimensional graphene foam loaded nickel-cobalt hydroxides nanoflakes and its electrochemical properties. *Electrochim Acta* 152:195–201



33. Guo H-L, Wang X-F, Qian Q-Y, Wang F-B, Xia X-H (2009) A green approach to the synthesis of graphene nanosheets. *ACS Nano* 3:2653–2659
34. Wang Z, Zhou X, Zhang J, Boey F, Zhang H (2009) Direct electrochemical reduction of single-layer graphene oxide and subsequent functionalization with glucose oxidase. *J Phys Chem C* 113:14071–14075
35. Li S-J, Xing Y, Deng D-H, Shi M-M, Guan P-P (2015) A comparative study of different types of reduced graphene oxides as electrochemical sensing platforms for hydroquinone and catechol. *J Solid State Electrochem* 19:861–870
36. Salimi A, Hallaj R, Soltanian S, Mamkhezri H (2007) Nanomolar detection of hydrogen peroxide on glassy carbon electrode modified with electrodeposited cobalt oxide nanoparticles. *Anal Chim Acta* 594:24–31
37. Salazar P, Rico V, Rodríguez-Amaro R, Espinós JP, González-Eliphe AR (2015) New copper wide range nanosensor electrode prepared by physical vapor deposition at oblique angles for the non-enzymatic determination of glucose. *Electrochim Acta* 169:195–201
38. Zhang D, Fang Y, Miao Z, Ma M, Du X, Takahashi S, J-i A, Chen Q (2013) Direct electrodeposition of reduced graphene oxide and dendritic copper nanoclusters on glassy carbon electrode for electrochemical detection of nitrite. *Electrochim Acta* 107:656–663
39. Li S-J, Du J-M, Zhang J-P, Zhang M-J, Chen J (2014) A glassy carbon electrode modified with a film composed of cobalt oxide nanoparticles and graphene for electrochemical sensing of H<sub>2</sub>O<sub>2</sub>. *Microchim Acta* 181:631–638
40. Shi J, Claussen JC, McLamore ES, Haque AU, Jaroch D, Diggs AR, Calvo-Marzal P, Rickus JL, Porterfield DM (2011) A comparative study of enzyme immobilization strategies for multi-walled carbon nanotube glucose biosensors. *Nanotechnology* 22:355502
41. Zhang Y, Xu F, Sun Y, Shi Y, Wen Z, Li Z (2011) Assembly of Ni(OH)<sub>2</sub> nanoplates on reduced graphene oxide: a two dimensional nanocomposite for enzyme-free glucose sensing. *J Mater Chem* 21:16949–16954
42. Wang X, Hu C, Liu H, Du G, He X, Xi Y (2010) Synthesis of CuO nanostructures and their application for nonenzymatic glucose sensing. *Sens Actuators B Chem* 144:220–225
43. Lee KK, Loh PY, Sow CH, Chin WS (2012) CoOOH nanosheets on cobalt substrate as a non-enzymatic glucose sensor. *Electrochem Commun* 20:128–132
44. Xia C, Ning W (2010) A novel non-enzymatic electrochemical glucose sensor modified with FeOOH nanowire. *Electrochem Commun* 12:1581–1584
45. Zhang J, Ma J, Zhang S, Wang W, Chen Z (2015) A highly sensitive nonenzymatic glucose sensor based on CuO nanoparticles decorated carbon spheres. *Sens Actuators B Chem* 211:385–391